Journal of Applied Automation Technologies

Research Paper

Improved Fault Diagnosis of Legged Robot Actuators Based on Feature Interaction-Aware LightGBM

Hanna Natasza Kostecka[1], Anna Kamila Jaworska[1] and Remigiusz Pajor[2, *]

[1] Faculty of Electrical Engineering, Automatics, Computer Science and Biomedical Engineering, Gdansk University of Technology, 80-233 Gdansk, Poland
[2] Maria Curie-Sklodowska University, Faculty of Mathematics, Physics and Computer Science, 20-031 Lublin, Poland
*Corresponding author: remigiusz.p@umcs.lublin.pl

Abstract. The initial drop in legged robot actuators is often masked by gait transitions, terrain changes, and various sensor noise sources, making it difficult to identify. Most conventional fault diagnosis models assume that input variables are independent, making it difficult to identify the coupled variations between current, torque, vibration, temperature, and joint tracking errors. To enhance actuator fault diagnosis, this paper proposes a LightGBM method based on feature interaction perception. Create a feature set related to gait for the actuators, determine the nonlinear interaction intensity between heterogeneous diagnostic variables, and incorporate this interaction information into the gradient boosting classifier. In the experiment, the actuator fault modes included torque loss, bearing wear, current anomalies, thermal drift, and composite material damage. The average inference time for each diagnostic window is 3.6 milliseconds, with an accuracy of 97.4%, a macro F1 score of 96.8%, and a weak fault recall rate of 94.9%. The above results indicate that feature learning based on interactive perception can enhance the ability to identify minor faults while reducing the computational cost of onboard health monitoring.

Keywords: *Weak Fault Diagnosis, Legged Robot, Actuator Degradation, LightGBM, Feature Interaction, Robust Classification*

Received on 13 April 2023, Accepted on 18 September 2023, Published on 29 September 2023

Introduction

Currently, quadruped robots are being used in applications such as inspection, rescue, mining, and logistics, where stable movement is required for wheeled platforms. The reliability of hip, knee, and ankle joint actuators is crucial, as they directly affect support, gait transitions, shock absorption, and posture recovery [1]. Legged robot actuators differ from traditional industrial actuators because they require frequent acceleration changes, terrain impacts, and periodic load reversals. Fault detection in multi-robot and mobile robot systems indicates that if early symptoms are not detected in a timely manner, actuator degradation may extend from local joints to overall body instability [2]. Moreover, research on the health monitoring of mobile robot actuators indicates that torque decay, current fluctuations, bearing wear, and temperature drift can all lead to changes in the motion behavior of mobile robot actuators [3].

Mechatronic systems and robots have already studied actuator fault diagnosis, but weak faults in legged robots are still difficult to distinguish from signal changes caused by normal gait. In joint servo systems, motor drivers, transmission mechanisms, reducers, encoders, and thermal protection units are all components that can generate electrical, mechanical, and control residual signals [4]. Quadruped robots can use lightweight hydraulic and series elastic actuators to improve vibration response, compliance, and load [5]. Current actuator diagnostic methods can use progressive diagnosis, sparse features, neural networks, or observer-based fault compensation. However, many methods still rely on manually isolating variables, without clearly representing the interactions between features [6]. The robot's current, torque, vibration, and joint tracking errors will change, and these

https://doi.org/10.64972/jaat.2023v1.306p20e:269-280

variables will all change simultaneously when transitioning from flat terrain to steep terrain or from a slow walk to steep terrain [7]. Therefore, robots cannot be classified independently [7]. According to fault-tolerant control research, delayed diagnosis increases recovery time and raises the risk of accidents [8].

This paper analyzes the fault diagnosis method for improved actuators of quadruped robots based on feature interaction-aware LightGBM. The method faces three practical issues: gait interference easily obscures weak fault features; heterogeneous actuator variables exhibit nonlinear interactions under load changes; and onboard diagnostics require low latency. First, create a feature representation coupled with the gait from temperature, vibration, torque, speed, current, and tracking error signals. Next, determine the interaction intensity between feature groups, and then add it to the LightGBM split optimization. Without reducing the efficiency of embedding inference, improve the fault category separation capability.

Related Work

Weak Fault Diagnosis in Robotic Actuators

Weak actuator failures typically manifest as slight changes in current waveforms, torque response, temperature rise, or increased vibration energy. These changes do not directly lead to shut down. Research on servo diagnostics of robotic joints indicates that damage to motor drivers, encoders, gearboxes, and transmission chains typically produces similar signals, especially during high-speed operation [9]. Research on service robots and quadrotor actuator failures indicates that the control loop can temporarily compensate for actuator anomalies, but performance faults can only be detected under such conditions [10]. Due to ground contact, gait phase switching, and continuously changing load conditions, quadruped robots are more significantly affected. During the swing phase, bearing failures or partial torque loss may occur, but this is almost nonexistent during the stance phase. It can encourage the creation of diagnostic models based on mechanical wear and other causes.

The diagnosis of motor electric actuators has shifted from threshold checks to data and model-driven learning. Progressive electro-hydraulic servo actuator diagnostics typically require accurate component models to distinguish between various fault stages [11]. The sparse feature LSTM method can improve the nonlinear representation of actuator signals. However, their inference costs and training dependencies make them unsuitable for airborne applications [12]. Due to their ability to handle various features and not requiring a large amount of memory to support deep networks, Random Forest, XGBoost, and Gradient Boosting are feasible machine learning models. Traditional tree models still only consider the individual feature that reduces impurity in the candidate split. The interaction changes between current fluctuations and torque lag, or the rise in temperature and gait load, are a few examples of weak faults. Therefore, the most obvious evidence of this splitting process may be overlooked.

Interaction-Aware Learning for Fault Classification

Due to the sensitivity of the original sensor sequence to sampling frequency, gait phase, and mechanical resonance, feature extraction of actuator faults is still needed to address the issue. Research on bearings and rotating machinery indicates that integrating time-domain, frequency-domain, and statistical indicators can improve diagnostic accuracy [13]. According to the feature ranking for brushless DC motor diagnosis and the subset selection for bearing diagnosis, compact features can reduce redundancy while maintaining fault sensitivity [14]. Robotics requires a similar approach, but the feature space should also include control variables, such as commanded torque, joint tracking error, support ratio, and load transfer. Since the variables are not independent, considering interaction selection methods is more appropriate than simple ranking.

LightGBM and other gradient boosting models have been used to diagnose faults in automotive systems, electrical equipment, bearings, gearboxes, and rotating machinery [15]. They have a tree structure that grows by leaves, flexible classification, and lower inference costs. Research on improved LightGBM and CNN-LightGBM shows that when fault-sensitive features are accurately represented, the boosting model can achieve high accuracy [16]. Most diagnostic methods based on LightGBM currently use predefined features and do not rely on feature coupling to modify the splitting process. Research on ReliefF-XGBoost, feature selection, and deep feature fusion indicates that interaction information can enhance robustness to noise and variations in operating conditions [17]. Due to the fact that the same physical damage produces different signals at different times during gait, interactive perception learning is very suitable for the actuators of quadruped robots.

Interpretable and deployable diagnostic models have been a recent research focus. Deep learning can handle nonlinear patterns, but it usually requires a large amount of labeled data and is difficult to interpret in embedded controllers [18]. Due to open-set time series fault diagnosis and real-time automotive fault prediction, the deployment environment should have controllable false positives, stable latency, and important feature contribution analysis [19]. The integrated model of feature selection and optimization is an effective method to address the issues [20]. Research on deep rotating machinery diagnosis indicates that heterogeneous sensor fusion can enhance fault discrimination capability by integrating vibration, current, and speed signals [21]. Binary particle swarm optimization indicates that a compact feature set can improve the diagnostic sensitivity of motor faults [22]. When diagnosing permanent magnet synchronous motor faults, research indicates that rotor speed and fault frequency should be considered together, rather than separately [23]. Moreover, open-set time series diagnostics indicate that models trained solely on a closed fault set may be unreliable [24]. Real-time automotive fault prediction indicates that flow stability and latency are the practical goals of automotive diagnostics [25]. Research on heterogeneous data rolling bearings indicates that multi-channel learning can enhance the ability to adapt to changing operating conditions [26]. As mentioned earlier, feature fusion can reduce the impact of local noise on bearing diagnosis [27]. Adaptive learning for bearing faults indicates that domain transfer should be considered when operating conditions change [28]. End-to-end bearing diagnosis has high computational costs, but it provides a good deep baseline [29]. Motor diagnosis based on computer vision neural networks (CNN) can distinguish between actual deceleration and changes in operating conditions during speed variations [30]. Therefore, the LightGBM model with feature interaction perception can combine the diagnostic advantages of nonlinear feature coupling, improve tree efficiency, and optimize the interpretability of actuator features.

Methodology and Diagnostic Experiment Design

Gait-Coupled Actuator Feature Representation

The diagnostic sample is generated from synchronized actuator current, motor torque, joint velocity, surface temperature, vibration acceleration, command torque, and tracking error. Each signal is segmented by a sliding window of 0.5 s with 50% overlap, corresponding to approximately one half of a trot gait cycle at $1.2\ \mathrm{m/s}$. The window length is short enough for online warning and long enough to contain stance-swing transition information. To reduce gaitinduced aliasing, every window is attached with a phase descriptor estimated from foot contact and joint velocity.

$$z_k = [i_k, \tau_k, v_k, \theta_k, a_k, e_k, g_k]^T \qquad \text{Eq.(1)}$$

Here, i_k is phase current, τ_k is estimated output torque, v_k is joint velocity, θ_k is actuator temperature, a_k is vibration acceleration, e_k is joint tracking error, and g_k is gait phase encoding.

$$f_j = \left[\mu_j, \sigma_j, r_j, E_j, H_j, C_j\right] \qquad \text{Eq.(2)}$$

The terms denote mean value, variance, root amplitude, spectral energy, entropy, and command-response correlation. In the experimental dataset, 126 raw descriptors are generated from seven channels before interaction filtering.

$$\phi_k = \mathrm{softmax}\left(W_g[g_k, v_k, e_k] + b_g\right) \qquad \text{Eq.(3)}$$

The phase vector ϕ_k is used to reweight fault-sensitive features. This operation reduces false alarms caused by normal gait transition and improves weak-fault recall under uneven terrain walking.

Figure 1 shows the recommendations for gait coupling. It first displays synchronous current, torque, speed, temperature, vibration, and tracking error signals in the same diagnostic window. Then, it adds gait phase weighting to distinguish actuator changes related to faults from normal stance-swing fluctuations. Compared to the original heterogeneous sensor data, the structure can provide the classifier with a set of compressed, physically meaningful diagnostic descriptors.

https://doi.org/10.64972/jaat.2023v1.306p20e:269-280

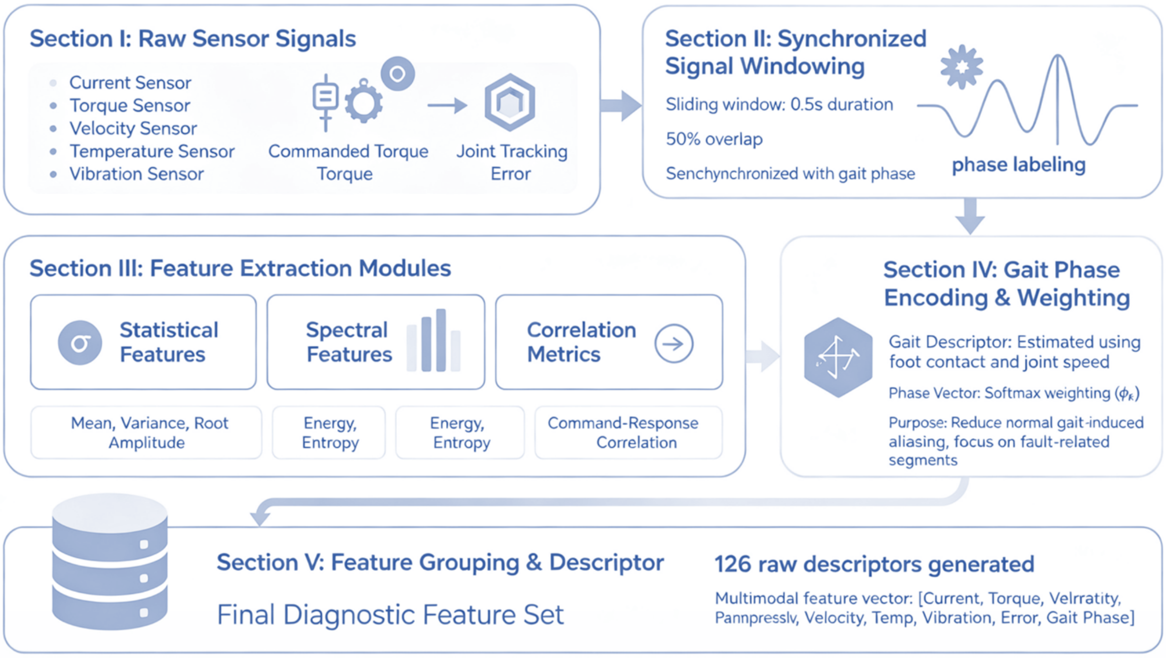

Figure 1. Gait-coupled actuator feature representation framework

Feature Interaction-Aware Fault Classification

Feature interaction is measured to identify coupled variables that jointly explain actuator degradation. The interaction matrix is computed from class-conditioned covariance, mutual separation, and local impurity reduction.

$$S_{ab} = \alpha I_{ab} + (1-\alpha)\Delta_{ab} \qquad \text{Eq.(4)}$$

In this expression, I_{ab} measures normalized dependence between feature a and feature b, while Δ_{ab} measures the change of class separation after the two features are combined.

$$q_a = \sum_b \frac{S_{ab}\pi_b}{1 + d_{ab}} \qquad \text{Eq.(5)}$$

The term π_b is the preliminary feature importance obtained by a shallow boosting model, and d_{ab} is the normalized redundancy distance.

$$\Gamma = \frac{G^2}{H+\lambda} + \eta q_a \qquad \text{Eq.(6)}$$

G and H are the first-order and second-order gradient statistics of the candidate split. The interaction correction increases the chance that weak but coupled features enter the tree.

$$\Omega_l = \gamma T_l + \lambda_l \|w_l\|_2^2 + \xi D_l \qquad \text{Eq.(7)}$$

T_l is the number of leaves, w_l is the leaf weight vector, and D_l denotes interaction density.

$$L = \sum_k CE(y_k, p_k) + \mu \left\| S - S_g \right\|_F^2 \qquad \text{Eq.(8)}$$

The model therefore learns a classifier that is sensitive to fault-related coupling but less sensitive to normal gait variation.

$$p_c = \frac{\exp(F_c(x))}{\sum_m \exp(F_m(x))} \qquad \text{Eq.(9)}$$

The delayed confirmation mechanism is useful for weak faults because a single abnormal window may come from ground impact.

$$A_k = \sum_{u=k-h}^{k} \omega_u p_c(x_u) \quad \text{Eq.(10)}$$

The accumulation horizon h is set to five windows, corresponding to about 1.5 s of motion.

The organizational structure of the interactive perception fault classification process from feature grouping to alarm output is shown in Figure 2. The confidence accumulation stage suppresses isolated anomaly windows caused by terrain influence or transient gait switching, while the interaction matrix guides LightGBM in the split selection of coupled actuator variables. Therefore, the model can enhance weak fault identification by reducing the complexity of deep sequence structures.

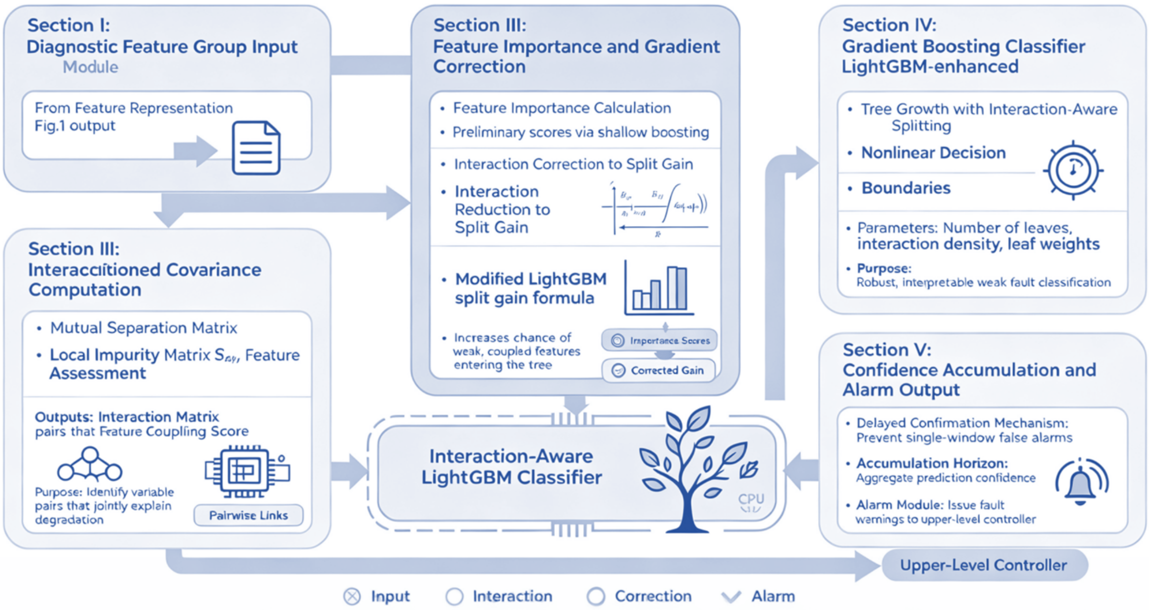

Figure 2. Interaction-aware fault classification process

Experimental Configuration and Evaluation Criteria

The quadruped robot joint actuator test platform is the foundation of the experimental dataset. Normal operation, torque loss, bearing wear, current anomalies, thermal drift, and compound degradation are the five fault modes.

$$w_c = \frac{N}{Cn_c} + \delta(1 - r_c) \quad \text{Eq.(11)}$$

Here, N is the total sample number, C is the class number, n_c is the number of samples in class c_r and r_c is the gaitphase coverage ratio.

$$M_{F1} = \frac{1}{C}\sum_{c} \frac{2P_cR_c}{P_c + R_c} \quad \text{Eq.(12)}$$

Macro-F1 is emphasized because class imbalance can hide poor weak-fault recognition.

$$R_w = \frac{TP_b + TP_t}{TP_b + FN_b + TP_t + FN_t} \quad \text{Eq.(13)}$$

Weak-fault recall is computed from bearing wear and thermal drift classes because these two faults have the smallest amplitude change in the early stage.

$$E_s = 0.6M_{F1} + 0.25R_w - 0.1L_n - 0.05M_n \quad \text{Eq.(14)}$$

L_n and M_n are normalized latency and model memory. With this criterion, the proposed model reaches an efficiency score of 0.921 on the validation set.

Result Analysis and Robustness Discussion

Weak Fault Recognition Performance

Figure 3 shows poor identification capability for inefficient actuators. As shown in Figure 3(a), the proposed model achieved a weak fault recall rate of 94.9%, which is higher than the 86.7% of standard LightGBM, 84.2% of Random Forest, 87.5% of XGBoost, 80.6% of MLP, and 82.1% of 1D CNN [31]. Figure 3(b) shows that this method reduces the false positive rate to 4.8%, compared to 7.6% for standard LightGBM and 9.1% for CNN. Figure 3(c) is the confusion matrix, where most of the remaining errors occur between early bearing wear and normal high-impact walking. The current-torque and vibration-speed interaction groups are the main new additions; therefore, even without a significant single-channel amplitude, weak degradation features can still be observed.

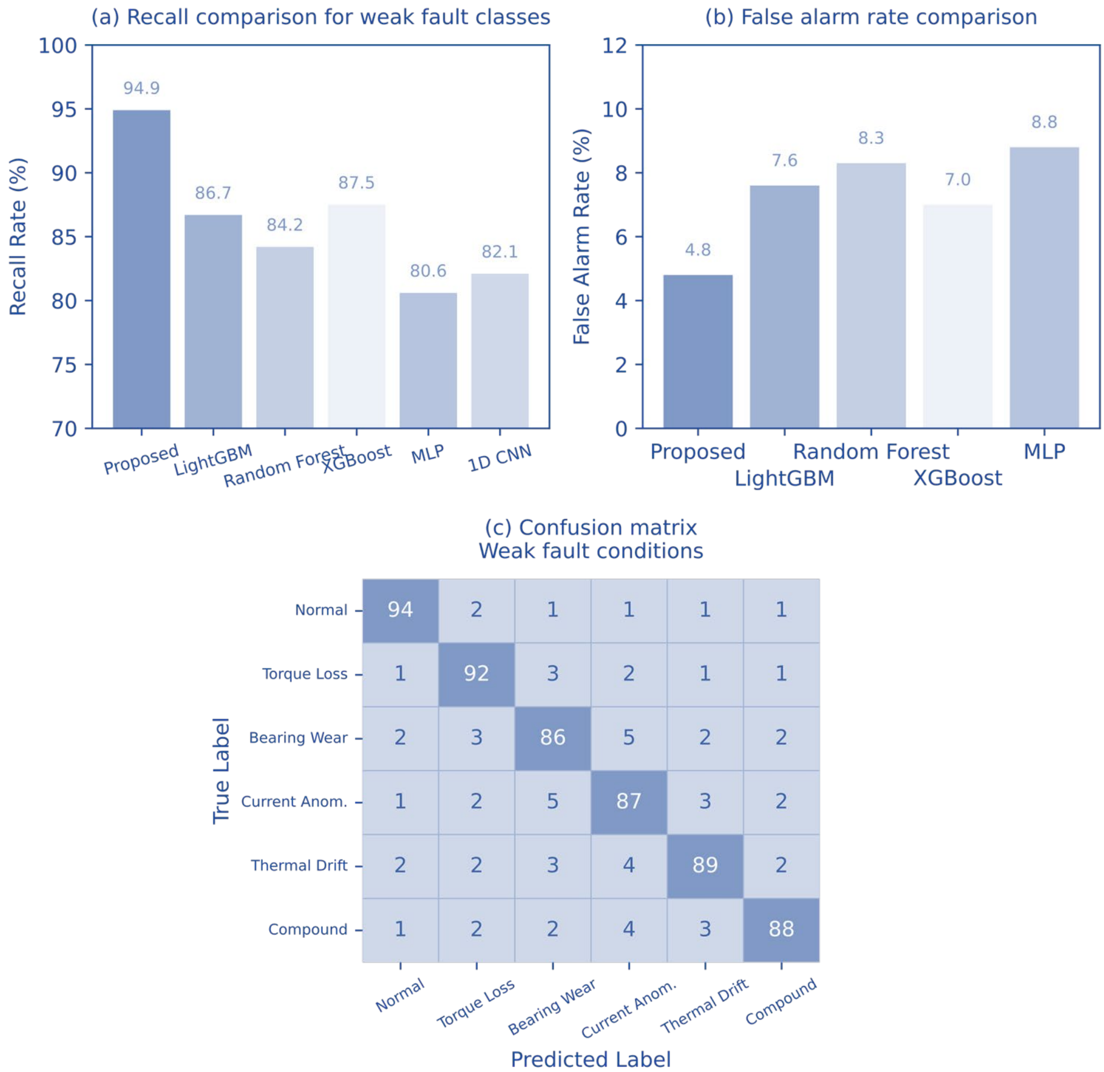

Figure 3. Weak actuator fault recognition performance. (a) Recall comparison for weak fault classes. (b) False alarm rate comparison. (c) Confusion matrix under weak fault conditions.

This situation is more pronounced during the minor fault stage. Under a 10% torque loss, the sample for the standard LightGBM is 88.3%, while the proposed model is 95.1%. On uneven ground, the recall rates of the bearings drop to 82.6% and 93.4%, respectively. The above findings indicate that when carefully selected fault-sensitive features are used, the performance of enhanced diagnostics is significantly better [32]. The new interaction patterns are still very small, adding coupled variables close to actuator degradation.

Feature Interaction and Diagnostic Separability

Feature interactions and separability are shown in Figure 4. As shown in Figure 4(a), the four strongest interactions are temperature-load, vibration-speed, torque-torque, and torque-error. Figure 4(b) shows the feature distribution of the standard LightGBM. In the low-dimensional projection, the normal samples of bearing wear and irregular terrain overlap. Figure 4(c) shows that the proposed model forms two smaller clusters for these two categories. Figure 4(d) shows that through interactive perception segmentation, the fault category boundaries are smoother near weak faults [33].

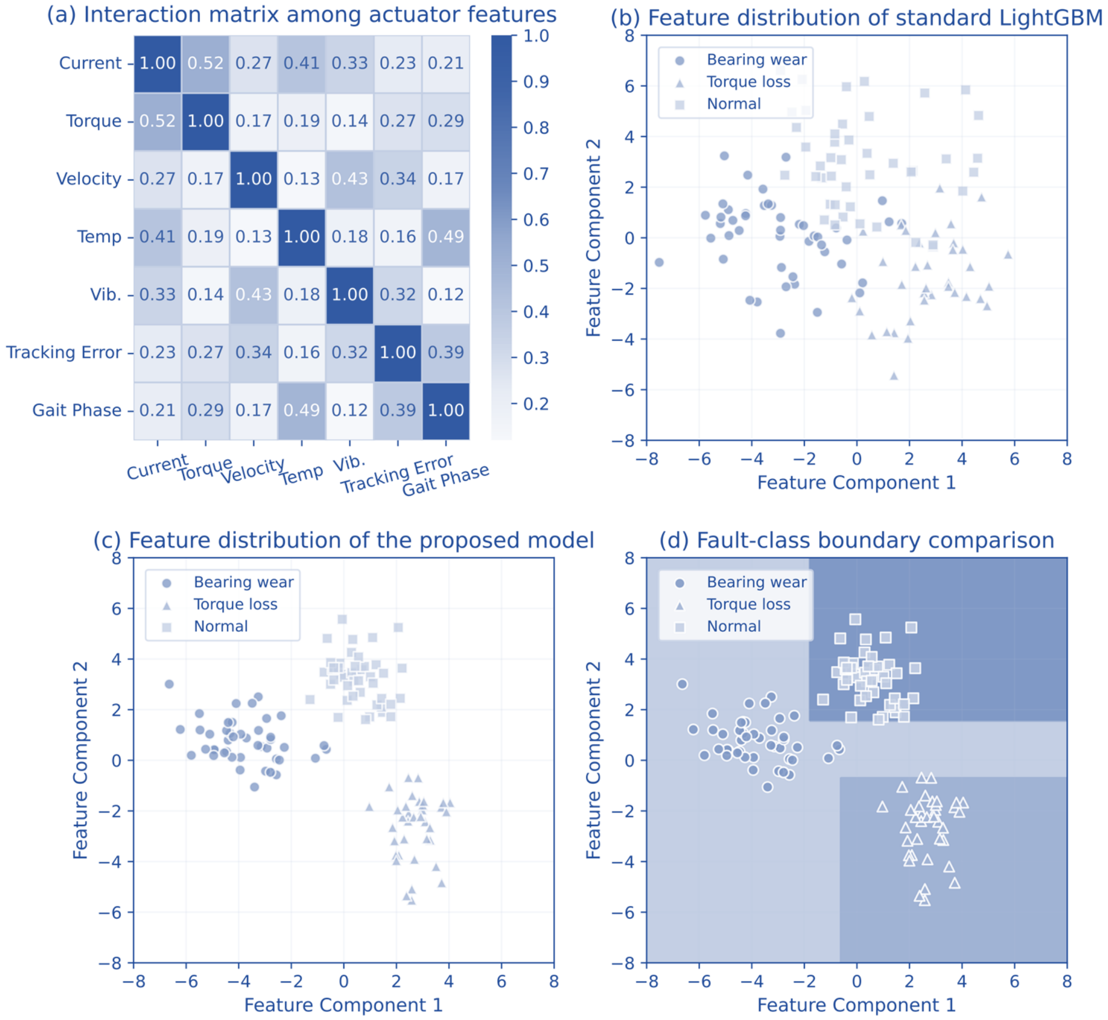

Figure 4. Feature interaction and separability visualization. (a) Interaction matrix among actuator features. (b) Feature distribution of standard LightGBM. (c) Feature distribution of the proposed model. (d) Fault-class boundary comparison.

Figure 5 is the decomposition of the feature groups. Figure 5(a) shows the classified interaction feature groups, where the current-torque coupling accounts for 21.4% of the total gain. Vibration-speed coupling accounts for 18.7%, and temperature-load coupling accounts for 15.2%. Figure 5(b) shows the change in accuracy after the feature group was excluded. Under the exclusion of the interaction between current and motor pairs, the overall F1 score decreased by 3.8 percentage points. In addition, addressing the temperature-load coupling issue can reduce the recovery of thermal deviation by 5 percentage points. 1 cent. These changes support the necessity of the relationship between cross variables for weak actuator diagnosis [34].

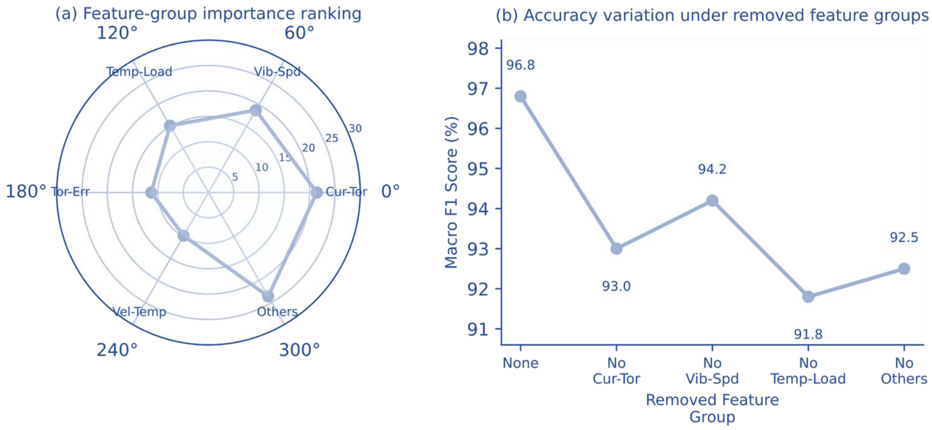

Figure 5. Contribution of interaction-aware feature groups. (a) Feature-group importance ranking. (b) Accuracy variation under removed feature groups.

Robustness and Generalization Analysis

Figure 6 shows the results of the robustness test under gait and sensor interference. As shown in Figure 6(a), after increasing the walking speed from 0.8 m/s to 1.6 m/s, the accuracy remains at 95.8%; however, the standard LightGBM drops to 92.4% [35]. Figure 6(b) shows the performance under the presence of sensor noise. When 8% Gaussian noise is added to the vibration and current channels, the macro F1 score only decreases by 1.9 percentage points. Load disturbance case Figure 6(c) shows a model that maintains a torque loss recall rate of over 94.0% under a 15% load variation. The gait condition interaction matrix reduces the likelihood of misinterpreting normal impact responses as degradation signals.

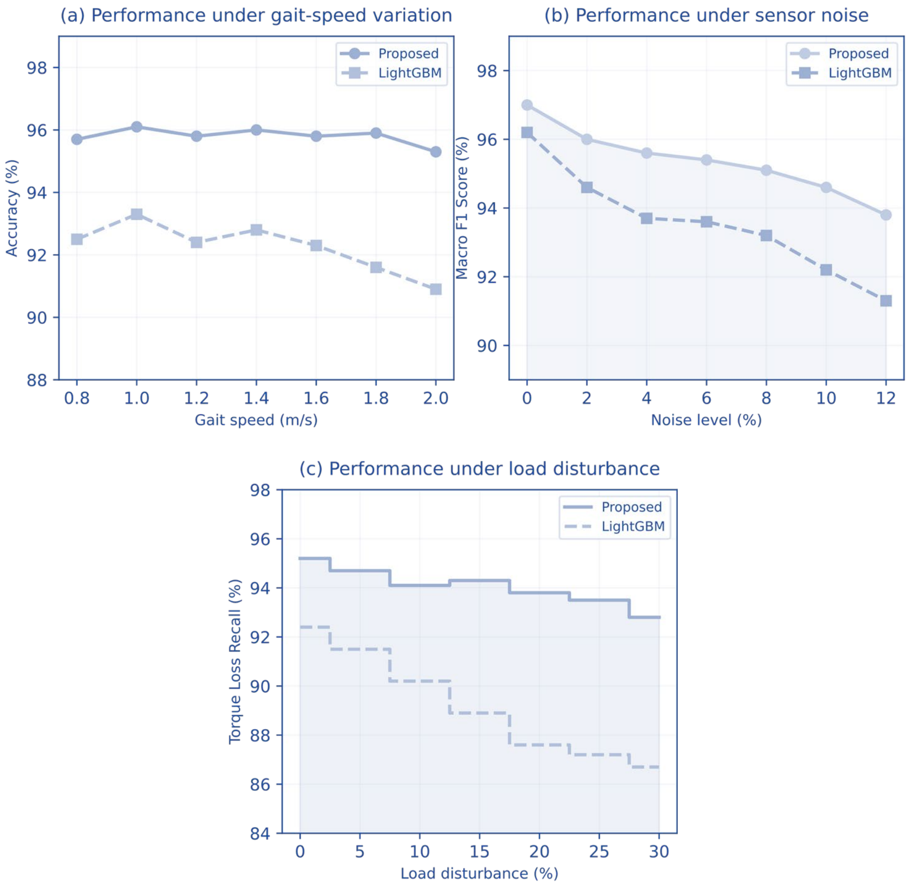

Figure 6. Robustness under gait and sensor disturbances. (a) Performance under gait-speed variation. (b) Performance under sensor noise. (c) Performance under load disturbance.

Figure 7 shows the deployment and generalization performance. Figure 7(a) shows the cross-condition diagnostic accuracy. After fine-tuning with only 12% of the labeled samples, the model achieved 93.6% on unseen terrain [36]. According to the inference latency shown in Figure 7(b), the proposed method has a latency of 3.6 milliseconds per window on an embedded CPU, which is lower than CNN (1.8 milliseconds) and XGBoost (4.2 milliseconds). The embedded deployment score in Figure 7(c) shows that the interaction-aware LightGBM is 0.917, higher than the standard LightGBM at 0.872 and the random forest at 0.846. Latency does not require offline, suitable for controlling supervisory-level monitoring actuators.

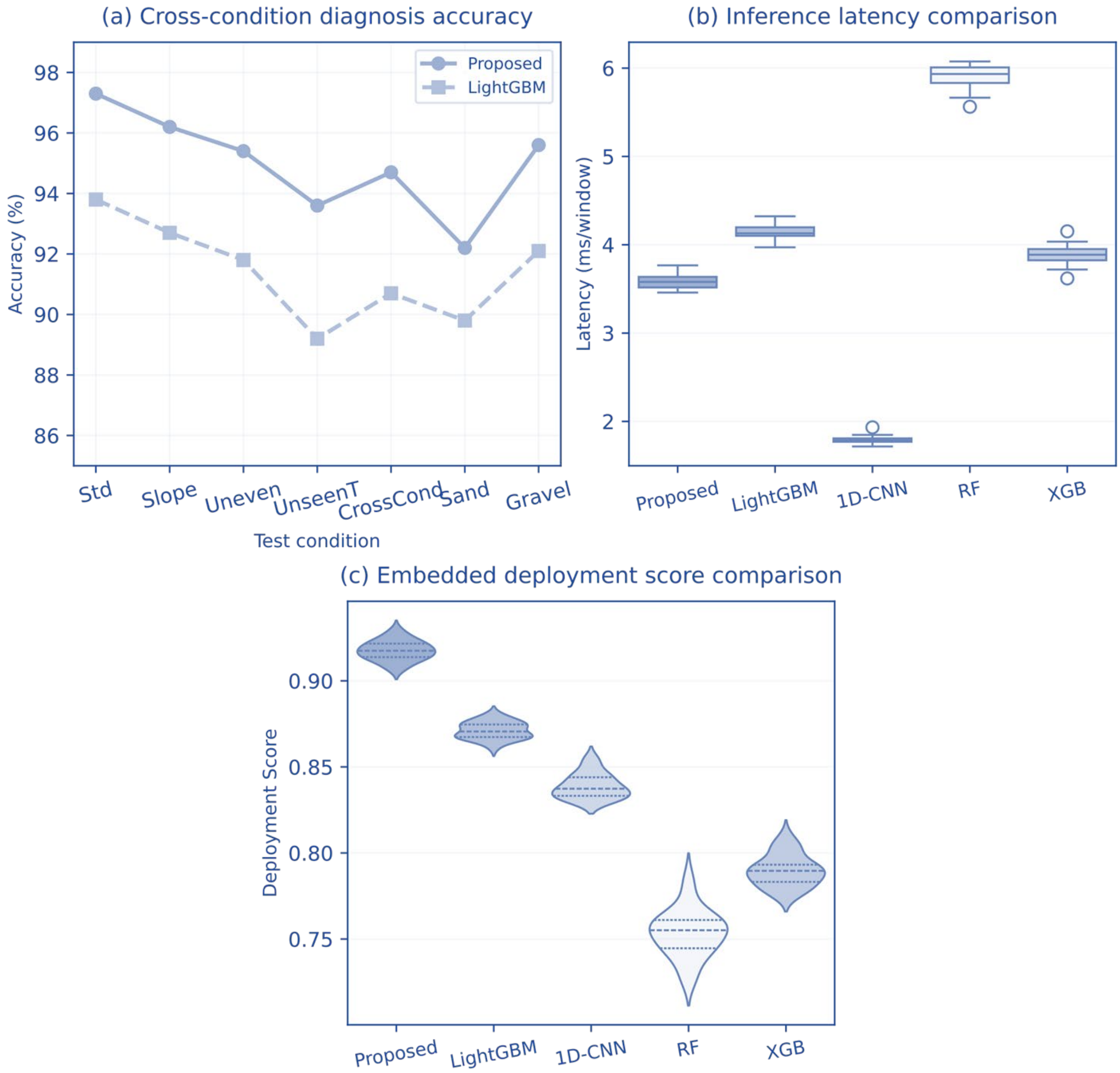

Figure 7. Generalization and deployment performance. (a) Cross-condition diagnosis accuracy. (b) Inference latency comparison. (c) Embedded deployment score comparison.

Furthermore, the results of the ablation experiment indicate that all parts are functioning normally. Due to the fact that slope walking samples are more difficult to distinguish than torque loss samples, reducing gait weighting decreased the accuracy from 97.4% to 95.6% [37]. After reducing the interaction perception split gain, the weak fault recall rate decreased from 94.9% to 89.9%. Due to the removal of confidence accumulation, the false positive rate increased from 4.8% to 6.9%. The proposed model offers more intuitive feature attribution and higher latency stability, but its representational capacity is inferior compared to the deep sequence baseline [38]. Quadruped robots need to operate onboard monitors with the help of motion control and perception modules [39]. Due to the combined degradation caused by simultaneous thermal drift and bearing wear, longer time series data or online adjustments may be required to eliminate the remaining errors [40].

Conclusion

This paper proposes a feature interaction-aware LightGBM method for identifying weak actuator faults in legged robots. The model uses tracking error signals, current, torque, speed, temperature, vibration, and gait-coupled actuator features to determine the nonlinear interaction intensity of heterogeneous variables. Adding interaction information in LightGBM split optimization to improve the model's representation of weak degradation patterns that are difficult to identify Through single-channel features.

According to the experiments, intervention-aware learning can improve diagnostic robustness and accuracy. The proposed method has a lower failure recall rate and a lower false positive rate. It is also more stable, even in the presence of variations in gait speed, sensor noise, terrain interference, and load changes. Deep sequence models require more computational resources than traditional sequence models. Therefore, due to inference latency and memory consumption, deep sequence models are not well-suited for embedded supervisory diagnostics on quadruped robot platforms.

In the future, these methods will be extended to online incremental updates, cross-robot transfer diagnosis, and integration with model-based actuator observers. More complex compound failures should also be considered, such as those involving thermal accumulation, control loop compensation, and mechanical wear simultaneously. In long-term field deployments, interactive perception enhancement and lifelong learning can extend the lifespan of actuator health monitoring.

Author Contributions

Hanna Natasza Kostecka contributes to conceptualization, methodology, software, validation, analysis, investigation, data collection, draft preparation, manuscript editing, visualization, supervision. Remigiusz Pajor contributes to analysis and investigation. Anna Kamila Jaworska contributes to methodology, software, validation and investigation. All authors have read and agreed with the manuscript before its submission and publication.

Funding

This research received no specific financial support from any funding agency.

Institutional Review Board Statement

Not applicable.

References

[1] Ma, L., Guo, J., Li, J., & Wang, J. (2022). A noise-excitation generative adversarial network for actuator fault diagnosis of multi-legged robot. Unmanned Systems, 11(2), 159-173. https://doi.org/10.1142/s2301385023410042
[2] Abci, B., El Najjar, M. E. B., & Cocquempot, V. (2019). Sensor and actuator fault diagnosis for a multi-robot system based on the Kullback-Leibler divergence. 2019 4th Conference on Control and Fault Tolerant Systems, 68-73. https://doi.org/10.1109/systol.2019.8864734
[3] Pan, J., Qu, L., & Peng, K. (2021). Sensor and actuator fault diagnosis for robot joint based on deep CNN. Entropy, 23(6), 751. https://doi.org/10.3390/e23060751
[4] Qi, H. T., Zhao, D. A., Liu, D., & Liu, X. (2022). Double redundancy electro-hydrostatic actuator fault diagnosis method based on progressive fault diagnosis method. Actuators, 11(9), 264. https://doi.org/10.3390/act11090264
[5] Abci, B., El Badaoui El Najjar, M., Cocquempot, V., & Dherbomez, G. (2019). An informational approach for sensor and actuator fault diagnosis for autonomous mobile robots. Journal of Intelligent & Robotic Systems, 99(2), 387-406. https://doi.org/10.1007/s10846-019-01099-7
[6] Wang, R., Zhao, J., & Wang, J. (2022). Torque compensation model and touchdown detection model of the hydraulic quadruped robot controlled by VMC. 2022 34th Chinese Control and Decision Conference, 3937-3943. https://doi.org/10.1109/ccdc55256.2022.10034130

[7] Farid, Y., & Ehsani-Seresht, A. (2021). Discrete finite-time robust fault-tolerant high-order sliding mode control of uncertain quadruped robot: An experimental assessment. International Journal of Intelligent Robotics and Applications, 5(1), 23-36. https://doi.org/10.1007/s41315-020-00161-0

[8] Nguyen, N. P., & Hong, S. K. (2019). Fault diagnosis and fault-tolerant control scheme for quadcopter UAVs with a total loss of actuator. Energies, 12(6), 1139. https://doi.org/10.3390/en12061139

[9] Kim, T., & Kim, S. (2022). Data-driven preflight diagnosis of hexacopter actuator fault based on principal component analysis of accelerometer signals. Lecture Notes in Networks and Systems, 378-385. https://doi.org/10.1007/978-3-030-97672-9_33

[10] Qiu, D., Sun, M., Fan, H., Shao, J., Lin, Y., & Huo, Z. (2021). Servo DC motor fault diagnosis driven by multi-source heterogeneous data. 2021 IEEE 10th Data Driven Control and Learning Systems Conference, 55-59. https://doi.org/10.1109/ddcls52934.2021.9455572

[11] Huang, J., Qi, L., Gu, J., Lu, Z., Sun, J., & Yu, C. (2021). Servo motor fault diagnosis based on data fusion. 2021 33rd Chinese Control and Decision Conference, 6737-6743. https://doi.org/10.1109/ccdc52312.2021.9602588

[12] Yang, J., Guo, Y., & Zhao, W. (2021). An intelligent fault diagnosis method for an electromechanical actuator based on sparse feature and long short-term network. Measurement Science and Technology, 32(9), 095102. https://doi.org/10.1088/1361-6501/abfbab

[13] Zhao, L., Wang, S., Shi, J., & Zhang, C. (2020). Fault diagnosis of hydraulic actuator based on improved convolutional neural network. 2020 Asia-Pacific International Symposium on Advanced Reliability and Maintenance Modeling, 1-6. https://doi.org/10.1109/aparm49247.2020.9209471

[14] Zhang, S., & Liu, Y. (2021). Fault diagnosis for the planetary gearbox based on an improved LightGBM. 2021 CAA Symposium on Fault Detection, Supervision, and Safety for Technical Processes, 1-6. https://doi.org/10.1109/safeprocess52771.2021.9693594

[15] Nemat Saberi, A., Belahcen, A., Sobra, J., & Vaimann, T. (2022). LightGBM-based fault diagnosis of rotating machinery under changing working conditions using modified recursive feature elimination. IEEE Access, 10, 81910-81925. https://doi.org/10.1109/access.2022.3195939

[16] Jia, X., Xiao, B., Zhao, Z., Ma, L., & Wang, N. (2021). Bearing fault diagnosis method based on CNN-LightGBM. IOP Conference Series: Materials Science and Engineering, 1043(2), 022066. https://doi.org/10.1088/1757-899x/1043/2/022066

[17] Xu, Y., Cai, W., Wang, L., & Xie, T. (2021). Intelligent diagnosis of rolling bearing fault based on improved convolutional neural network and LightGBM. Shock and Vibration, 2021, 1205473. https://doi.org/10.1155/2021/1205473

[18] Zhao, G., Zhang, Y., Wu, K., & Zhou, J. (2021). Rotating machinery fault diagnosis using light gradient boosting machine. 2021 Global Reliability and Prognostics and Health Management, 1-6. https://doi.org/10.1109/phm-nanjing52125.2021.9613088

[19] Zhu, Q. X., Zhang, N., He, Y. L., & Xu, Y. (2022). Novel imbalanced fault diagnosis method based on CSMOTE integrated with LSDA and LightGBM for industrial process. 2022 8th International Conference on Control, Decision and Information Technologies, 326-331. https://doi.org/10.1109/codit55151.2022.9803941

[20] Chai, L., Zhang, J., Shangguan, W., Xiao, X., Li, X., & Nie, M. (2022). CBTC on-board signal fault diagnosis method based on LightGBM classification. 2022 China Automation Congress, 4404-4409. https://doi.org/10.1109/cac57257.2022.10055845

[21] Li, Z., Hu, K., Chen, H., & Liu, Q. (2021). Fault diagnosis model of refrigeration system combining Boruta and LightGBM methods for energy saving. IOP Conference Series: Earth and Environmental Science, 675(1), 012196. https://doi.org/10.1088/1755-1315/675/1/012196

[22] Wu, Z., Wang, X., & Jiang, B. (2020). Fault diagnosis for wind turbines based on ReliefF and extreme gradient boosting. Applied Sciences, 10(9), 3258. https://doi.org/10.3390/app10093258

[23] Wang, Z., Huang, H., & Wang, Y. (2021). Fault diagnosis of planetary gearbox using multi-criteria feature selection and heterogeneous ensemble learning classification. Measurement, 173, 108654. https://doi.org/10.1016/j.measurement.2020.108654

[24] Buchaiah, S., & Shakya, P. (2022). Bearing fault diagnosis and prognosis using data fusion-based feature extraction and feature selection. Measurement, 188, 110506. https://doi.org/10.1016/j.measurement.2021.110506

[25] Lee, C. Y., & Hung, C. H. (2021). Feature ranking and differential evolution for feature selection in brushless DC motor fault diagnosis. Symmetry, 13(7), 1291. https://doi.org/10.3390/sym13071291

[26] Saha, D. K., Hoque, M. E., & Badihi, H. (2022). Development of intelligent fault diagnosis technique of rotary machine element bearing: A machine learning approach. Sensors, 22(3), 1073. https://doi.org/10.3390/s22031073
[27] Nakamura, H., & Mizuno, Y. (2022). Diagnosis for slight bearing fault in induction motor based on combination of selective features and machine learning. Energies, 15(2), 453. https://doi.org/10.3390/en15020453
[28] Luo, J., Zhu, L., Li, Q., Liu, D., & Chen, M. (2021). Imbalanced fault diagnosis of rotating machinery based on deep generative adversarial networks with gradient penalty. Processes, 9(10), 1751. https://doi.org/10.3390/pr9101751
[29] Brito, L. C., Susto, G. A., Brito, J. N., & Duarte, M. A. (2022). An explainable artificial intelligence approach for unsupervised fault detection and diagnosis in rotating machinery. Mechanical Systems and Signal Processing, 163, 108105. https://doi.org/10.1016/j.ymssp.2021.108105
[30] Apley, D. W., & Zhu, J. (2020). Visualizing the effects of predictor variables in black box supervised learning models. Journal of the Royal Statistical Society Series B: Statistical Methodology, 82(4), 1059-1086. https://doi.org/10.1111/rssb.12377
[31] Lundberg, S. M., Erion, G., Chen, H., DeGrave, A., Prutkin, J. M., Nair, B., et al. (2020). From local explanations to global understanding with explainable AI for trees. Nature Machine Intelligence, 2(1), 56-67. https://doi.org/10.1038/s42256-019-0138-9
[32] Barredo Arrieta, A., Díaz-Rodríguez, N., Del Ser, J., Bennetot, A., Tabik, S., Barbado, A., et al. (2020). Explainable artificial intelligence: Concepts, taxonomies, opportunities and challenges toward responsible AI. Information Fusion, 58, 82-115. https://doi.org/10.1016/j.inffus.2019.12.012
[33] Matzka, S. (2020). Explainable artificial intelligence for predictive maintenance applications. 2020 Third International Conference on Artificial Intelligence for Industries, 69-74. https://doi.org/10.1109/ai4i49448.2020.00023
[34] Zeng, W., Davoodi, A., & Topaloglu, R. O. (2020). Explainable DRC hotspot prediction with Random Forest and SHAP tree explainer. 2020 Design, Automation & Test in Europe Conference & Exhibition, 1151-1156. https://doi.org/10.23919/date48585.2020.9116488
[35] Cao, B., & Yao, L. (2022). Fault diagnosis for bilinear stochastic distribution systems with actuator fault. 2022 IEEE 20th International Conference on Industrial Informatics, 718-722. https://doi.org/10.1109/indin51773.2022.9976169
[36] Yang, R., & Zhong, M. (2022). Fault diagnosis method based on recurrent convolutional neural network. Machine Learning-Based Fault Diagnosis for Industrial Engineering Systems, 11-25. https://doi.org/10.1201/9781003240754-2
[37] Simani, S., & Castaldi, P. (2021). Nonlinear methods for fault diagnosis. Diagnosis and Fault-Tolerant Control 2, 1-56. https://doi.org/10.1002/9781119882350.ch1
[38] Wang, Z., & Yao, L. (2021). Fault diagnosis and fault-tolerant control for non-linear UAV system subject to sensor and actuator faults. 2021 40th Chinese Control Conference, 4368-4373. https://doi.org/10.23919/ccc52363.2021.9549459
[39] Zhou, S., Guo, K., Yu, X., Guo, L., & Zhang, Y. (2021). Quadrotor actuator fault diagnosis and accommodation based on nonlinear adaptive state observer. Fault Diagnosis and Prognosis Techniques for Complex Engineering Systems, 305-326. https://doi.org/10.1016/b978-0-12-822473-1.00002-1
[40] Dong, J., Wang, J., & Guo, R. (2019). Remaining useful life prognostics for the electro-hydraulic actuator using relevance vector machine and optimized on-line incremental learning. MATEC Web of Conferences, 277, 02009. https://doi.org/10.1051/matecconf/201927702009